APPLIED AND ENVIRONMENTAL MICROBIOLOGY, Mar. 2007, p. 1968–1975 Vol. 73, No. 6
0099-2240/07/$08.00+0 doi:10.1128/AEM.02292-06


# Zooxanthellae Harvested by Ciliates Associated with Brown Band Syndrome of Corals Remain Photosynthetically Competent▽

Karin E. Ulstrup,[1,2] Michael Kühl,[3] and David G. Bourne[2]*

*Institute for Water and Environmental Resource Management and Department of Environmental Science, University of Technology, Sydney, P.O. Box 123, Broadway, New South Wales 2007, Australia[1]; Australian Institute of Marine Science, PMB No. 3, Townsville MC 4810, Queensland, Australia[2]; and Marine Biological Laboratory, Institute of Biology, University of Copenhagen, Strandpromenaden 5, DK-3000 Helsingør, Denmark[3]*

Received 28 September 2006/Accepted 18 January 2007

**Brown band syndrome is a new coral affliction characterized by a local accumulation of yet-unidentified ciliates migrating as a band along the branches of coral colonies. In the current study, morphologically intact zooxanthellae (= *Symbiodinium*) were observed in great numbers inside the ciliates (>50 dinoflagellates per ciliate). Microscale oxygen measurements and variable chlorophyll *a* fluorescence analysis along with microscopic observations demonstrated that zooxanthellae within the ciliates are photosynthetically competent and do not become compromised during the progression of the brown band zone. Zooxanthellae showed similar trends in light acclimation in a comparison of rapid light curve and steady-state light curve measures of variable chlorophyll *a* fluorescence. Extended light exposure of steady-state light curves resulted in higher quantum yields of photosystem II. The brown band tissue exhibited higher photosynthetically active radiation absorptivity, indicating more efficient light absorption due to a higher density of zooxanthellae in the ciliate-dominated zone. This caused relatively higher gross photosynthesis rates in the zone with zooxanthella-containing ciliates compared to healthy coral tissue. The observation of photosynthetically active intracellular zooxanthellae in the ciliates suggests that the latter can benefit from photosynthates produced by ingested zooxanthellae and from photosynthetic oxygen production that alleviates diffusion limitation of oxic respiration in the densely populated brown band tissue. It remains to be shown whether the zooxanthellae form a stable symbiotic association with the ciliate or are engulfed incidentally during grazing on coral tissue and then maintained as active inside the ciliate for a period before being digested and replaced by new zooxanthellae.**

A recently identified coral disease, brown band syndrome (BrB), was described for the first time in three coral families (Acroporidae, Pocilloporidae, and Faviidae) in the northern and southern sectors of the Great Barrier Reef (GBR), Australia (55). Macroscopic symptoms of the syndrome manifest as a brown zone on the coral preceded by healthy tissue and followed by exposed white skeleton (see Fig. 1A). Sometimes, a white zone is observed between the brown band and healthy tissue which may comprise bleached tissue and/or denuded skeleton (55). Microscopic investigations of the brown zone revealed the massive presence of an unknown protozoan ciliate which accumulates zooxanthellae intracellularly, resulting in the characteristic brown coloring of the observed syndrome. The ciliate band has been observed to migrate along the length of branching corals from base to tip at a rapid rate (>5 cm per day [B. Willis, personal communication]). The ciliates appear to ingest coral tissue at the lesion interface, accumulating the symbiotic dinoflagellates, known as zooxanthellae (= *Symbiodinium*), from the coral endoderm. However, it is unknown whether the zooxanthellae remain photosynthetically active inside the ciliates.

In this study, we used variable chlorophyll *a* fluorescence analysis with Mini- and Imaging-PAM (pulse-amplitude-modulation) instruments (22, 23, 37) and the saturation-pulse technique (reviewed in reference 45) to obtain measures of maximum and effective quantum yields of photosystem II (PSII) and derived measures of photosynthetic electron transport (24, 36). These measurements were combined with oxygen microelectrodes (25, 53) to assess the photosynthetic competency of zooxanthellae of corals affected with BrB. The combination of their fast response times, small tip diameters, and extremely small oxygen consumption means that $O_2$ microsensors are able to measure rapid changes in oxygen depletion as well as microprofiling of the diffusion boundary layer (DBL) (required to measure net photosynthesis and dark-respiration rates) at a spatial resolution of better than 100 μm and with response times of <0.2 to 0.5 s (26, 40, 53).

Only a limited number of studies have examined coral-protozoan associations (1, 2, 7, 29, 30, 47, 56). In this study, we compare the photosynthetic performances of zooxanthellae in healthy tissue preceding the brown band zone and within ciliates accumulating in the brown band zone of affected *Acropora muricata* corals. Direct microscopic and histological observations combined with photophysiological responses were analyzed to determine the competency of internalized zooxanthellae. Our results show that the dynamics of photosynthesis regulation of visually healthy zooxanthellae accumulated in the brown band zone were greatly altered (as shown by $O_2$-derived measures) from that of zooxanthellae in the healthy tissue. Nevertheless, the capacity for photosynthesis appeared unchanged (as shown by variable chlorophyll *a* fluorescence-derived measures).

* Corresponding author. Mailing address: Australian Institute of Marine Science, PMB 3, Townsville MC 4810, QLD, Australia. Phone: 61 7 4753 4139. Fax: 61 7 4772 5852. E-mail: d.bourne@aims.gov.au.
▽ Published ahead of print on 26 January 2007.

## MATERIALS AND METHODS

**Sampling.** Specimens of the branching coral *Acropora muricata* exhibiting symptoms of BrB were collected in November 2005 from an exposed reef flat at Davies Reef (18°49.86′S, 147°38.2′E) on the GBR and brought to the facilities of the Australian Institute of Marine Science in Townsville for further analysis.

**Histological and microscopic examination.** For histological examination, the brown band mass including ciliates and coral tissue was scraped from a coral branch and concentrated by centrifugation (1,000 × *g*) with excess liquid removed. Samples were fixed in Davidson's fixative (21) for 24 h prior to processing. All samples were sectioned (5 μm) and stained (Mayer's hematoxylin and eosin) using routine histological procedures and examined using light microscopy (3). Microscopic visualization was performed with a Zeiss Axioskop II microscope (Carl Zeiss, Jena, Germany) with images captured by an AxioCam MRC5 (Zeiss) high-resolution, cooled charge-coupled device camera. Fluorescence images were obtained using a halogen lamp for incident light and a Cy3 filter set, HQCy3 (excitation, BP535/50 nm; dichroic mirror, Q565 LP; emission, BP610/75 nm) (Carl Zeiss, Jena, Germany).

**PAR Abs and chlorophyll *a* determinations.** The Imaging-PAM estimates photosynthetically active radiation (PAR) absorptivity (Abs), i.e., the fraction of incident PAR that is absorbed, from the ratio of reflectance of red light (650 nm) (R) to the reflectance of nonabsorbed near-infrared light (780 nm) (NIR) from the tissue surface:

$$\text{Abs} = 1 - (\text{R}/\text{NIR}) \quad (1)$$

This parameter was measured in both the healthy and brown band tissue of each replicate coral colony. It is important to note that Abs estimates the light absorption via reflectance from a surface. Highly pigmented tissue surfaces will thus show higher absorptivity than surfaces with pigments distributed more homogeneously or deeper in the tissue although the overall chlorophyll concentration may be the same.

Tissue derived from ~1 $cm^2$ of healthy and brown band tissue, respectively, was extracted in 1 ml of methanol for 2 h. Extracts were centrifuged (15,000 rpm) for 2 min, and the clarified supernatant was mixed 1:1 in 70:30 (vol/vol) methanol-28 mM aqueous tetrabutyl ammonium acetate, pH 6.5. A 5-μl sample of the mixture was injected onto a Phenomenex $C_8$ column (3-μm particle size, 50 × 4.6 mm) at room temperature (21°C). Analysis was performed by reverse-phase high-performance liquid chromatography on a personal computer-interfaced high-performance liquid chromatography system (Waters Corporation). System control, data collection, and integration were performed using Empower Pro software (Waters Corporation, 2002). Pigments were separated using a binary mobile phase system, 70:30 (vol/vol) methanol-28 mM aqueous tetrabutyl ammonium acetate, pH 6.5 (75% to 100%), over 10 min. The flow rate was kept constant at 1 ml $min^{-1}$. Chlorophyll *a* was detected using a photodiode array detector, and pigment identity was determined through spectral comparison to a chlorophyll *a* standard (Sigma-Aldrich). The height (h) and radius (r) of the cylinder-shaped and fingertip-sized coral pieces, from which tissue was extracted, were measured to the nearest mm using calipers and applied to the formula for calculating the lateral surface area of a cylinder ([2 × π × r] × h). The surface area was calculated excluding the top and base, since these represented the area of attachment to the colony and therefore had no surface tissue.

**Combined measures of variable chlorophyll *a* fluorescence and $O_2$ productivity.** In order to assess the photosynthetic activity of zooxanthellae, three or four *Acropora muricata* branches from separate coral colonies showing symptoms of BrB were measured. The following setup and measuring sequence were applied to each colony: once in the asymptomatic healthy tissue 4 to 5 cm away from the lesion and once in the center (most dense region) of the brown band zone.

An initial rapid light curve (RLC) with 10-second intervals between irradiances (0, 1, 73, 144, 365, 515, 690, 911, and 1204 μmol photons $m^{-2}$ $s^{-1}$) was performed on a dark-acclimated coral using the Imaging-PAM fluorometer (Walz, Effeltrich, Germany). For oxygen microelectrode measurements, the coral was then placed in a custom-built flow chamber (25 × 10 × 10 cm) through which seawater from a reservoir was circulated at a flow velocity of ~1 cm $s^{-1}$. The reservoir contained approximately 20 liters of seawater and was maintained at 27 ± 0.5°C using a glass aquarium heater (100 W; Aqua One; Kong's International, Australia).

An $O_2$ microelectrode (39), which was linearly calibrated by recording signals in air-saturated seawater and $O_2$-free seawater, was positioned at an angle of 25° relative to the light source (Schott 2500), while the coral sample was observed with a dissecting microscope (Leica, Germany). The microsensor was placed in direct contact with the coral tissue surface by using a manually operated micromanipulator (MM33; Märtzhäuser, Germany), and the measuring signal was recorded via a picoamperemeter (PA2000; Unisense A/S, Denmark) on a strip-chart recorder (Kipp & Zonen, The Netherlands). Corals were illuminated with a fiber-optic tungsten-halogen light source with a collimating lens (Schott KL-2500; Germany) that was calibrated against a light sensor (LI-192SB; LI-COR). Each irradiance (0, 33, 59, 91, 130, 247, 494, and 845 μmol photons $m^{-2}$ $s^{-1}$) was applied for 10 min in order to obtain steady-state conditions prior to $O_2$ measurements (53). At steady state for a particular irradiance $O_2$ transport, consumption, and production are in equilibrium and no changes to the $O_2$ level are detected over time (26). Monitoring of the tissue surface oxygen level on the strip-chart recorder after adjustments of irradiance showed that 10 min was sufficient to reach steady state.

Oxygen microprofiles in darkness were measured in vertical steps of 10 μm from the tissue surface through the DBL and out into the bulk water, which had a constant oxygen content (tabulated value of 204.3 μmol $O_2$ $liter^{-1}$ at 27°C and salinity of 35 ppt; Unisense). The oxygen flux (dark-respiration rate) was calculated from the oxygen concentration profile as

$$J = -D_o \times \text{dC}/\text{dz} \quad (2)$$

where $D_o$ is the diffusion coefficient of $O_2$ at 27°C and salinity of 35 ppt (tabulated value, $2.35 \times 10^{-5}$ $cm^2$ $s^{-1}$; Unisense) and dC/dz is the constant slope of the oxygen gradient in the DBL; this calculation assumes a one-dimensional diffusion geometry (25).

At each following irradiance level (33, 59, 91, 130, 247, 494, and 845 μmol photons $m^{-2}$ $s^{-1}$), the microelectrode tip was positioned at the tissue surface, and when steady-state oxygen conditions were verified, a sudden and brief (1- to 3-s) light-dark shift was performed to estimate gross photosynthesis rate (26, 53). The light-dark shift technique, which requires steady-state $O_2$ distribution before the light-dark shift, enables the measurement of gross photosynthesis rate as the immediate rate of oxygen depletion after onset of darkness (more details in reference 40). After gross photosynthesis measurements, oxygen microprofiles were measured and used to estimate net photosynthesis rates by equation 2. Finally, the Mini-PAM fluorometer (Walz, Effeltrich, Germany) fitted with a 2-mm fiber-optic probe was used at each irradiance level for an effective quantum yield ($\Delta F/F_m'$) reading using a single saturating flash. The probe was gently hand held to the surface of the coral adjacent to the $O_2$ microsensor. These measurements were used to generate a steady-state light curve (SSLC) of relative electron transport rate (rETR) versus irradiance.

The initial RLC using the Imaging-PAM was repeated at the highest irradiance level (845 μmol photons $m^{-2}$ $s^{-1}$). In order to maintain the high-light-acclimated state of PSII, actinic light (845 μmol photons $m^{-2}$ $s^{-1}$) was turned on for 1 min after the coral was positioned in the Imaging-PAM prior to initiation of the RLC. The first saturating flash in the dark-acclimated RLC provided a measure of maximum quantum yield ($F_v/F_m$), which was compared to the first measure of the light-acclimated RLC, which provided a comparative $\Delta F/F_m'$ (845 μmol photons $m^{-2}$ $s^{-1}$). The maximum excitation pressure over PSII was then calculated as $Q_m = 1 - [(\Delta F/F_m')/(F_v/F_m)]$ (24). $Q_m$ is used as a proxy for the physiological performance of the zooxanthellae, where values close to 0 indicate that photosynthesis is light limited even at high irradiance, while values closer to 1 indicate closure of PSII at high irradiance, e.g., due to photoinhibition.

The rETR derived from the RLCs as well as from the steady-state light curves was calculated as $\text{rETR} = \Delta F/F_m' \times \text{PAR}$, where $\Delta F/F_m' = (F_m' - F_t)/F_m'$ (45). The light curves (both fluorescence and $O_2$ derived) were subsequently fitted to the formula of Platt et al. (35), whereby quantitative parameters of $\text{rETR}_{\text{max}}$ or $P_{g,\text{max}}$ (maximum gross photosynthesis rate), α (light utilization coefficient), and $E_k$ (minimum saturating irradiance) were calculated (details are in references 27 and 36).

**Statistical analysis.** One-way analysis of variance tests (SPSS v11.0.0) were used to determine if significant differences in the following parameters were present between healthy and brown band tissue: $F_v/F_m$, $\Delta F/F_m'$, $Q_m$, quantitative parameters of RLCs and steady-state light curves (fluorescence and $O_2$ derived), PAR absorptivity, and chlorophyll *a* content. Where the assumptions of normality and equal variance failed ($P < 0.05$), data were transformed using natural log; this applied only to $\text{rETR}_{\text{max}}$ values for RLCs and SSLCs. Transformed data successfully met the assumptions of normality and equal variance. Post hoc comparisons were performed on quantitative parameters of RLCs and fluorescence derived steady-state light curves using the Tukey-Kramer honestly significant difference test.

## RESULTS

**Field and microscopic observations of BrB.** BrB exhibits distinctive macroscopic symptoms in the field (Fig. 1A), which

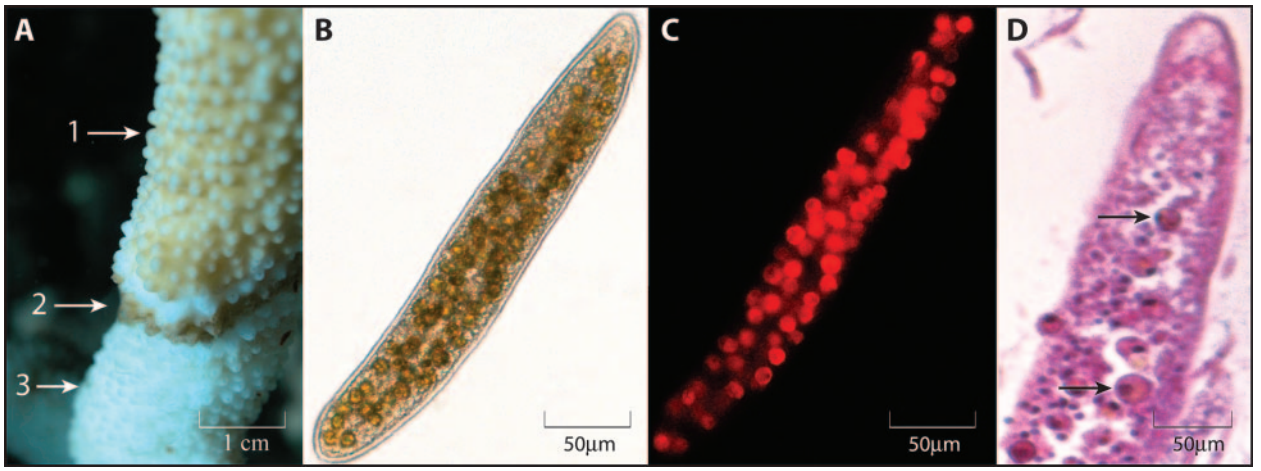


FIG. 1. (A) BrB on an *Acropora muricata* branch at Davies Reef showing the macroscopic field signs of this syndrome including (1) healthy coral tissue preceding the brown band zone, (2) the brown zone of accumulated ciliates, and (3) exposed white coral skeleton following the brown zone (photograph by Cathie Page). (B) Brown band ciliate morphology as examined under a high-power compound microscope (magnification, ×100), demonstrating zooxanthellae within the ciliate. (C) Brown band ciliate from panel B under green excitation light, demonstrating autofluorescence of internalized zooxanthellae. (D) Histopathological micrograph of a transverse section of a brown band ciliate. Arrows highlight internalized zooxanthellae within the ciliate with dark patches within zooxanthellae being stained chromosomal DNA.

are derived from ciliates gliding over the exterior of the coral samples and into the coelenteron and cavities of the coral polyps. Light microscopic analysis of the ciliates demonstrated an accumulation of intact zooxanthellae within the ciliates (Fig. 1B). The ingested zooxanthellae maintained a strong localized chlorophyll autofluorescence, indicating intact chloroplasts and a potential capacity for photosynthesis (Fig. 1C). In addition, histological cross sections of the sampled brown band mass demonstrated that the ciliates contained intact zooxanthellae that were not surrounded by food vacuoles (Fig. 1D).

**PAR absorptivity and chlorophyll *a* determinations.** Variable chlorophyll *a* fluorescence imaging showed high fluorescence along with high PAR absorptivity in the brown band tissue (Fig. 2A and C), and active photosynthesis in the brown band tissue was evident by a maximum quantum yield ($F_v/F_m$) comparable to or slightly higher than that in the healthy tissue (Fig. 2B).

Measurements of PAR absorptivity were significantly lower ($P = 0.001$) in the healthy tissue (0.304 ± 0.02) than in the brown band tissue (0.592 ± 0.03) (Fig. 3). However, chlorophyll *a* content in the healthy tissue (2.22 ± 1.79 μg/cm$^2$ surface area) was not significantly different ($P = 0.904$) from the content found in brown band tissue (1.92 ± 1.55 μg cm$^2$ sur-

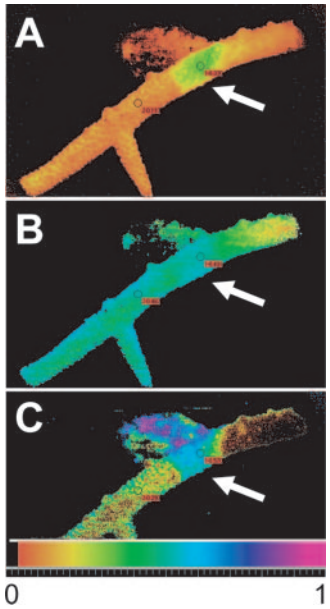


FIG. 2. Variable chlorophyll *a* fluorescence imaging of an *Acropora muricata* branch with brown band syndrome (marked with arrow). (A) Chlorophyll *a* fluorescence ($F_o$) of the brown band tissue shows higher values than that of the healthy coral tissue on the left-hand side of the band. (B) Maximum quantum yield ($F_v/F_m$) of PSII. C. Absorptivity of PAR. All pictures are color coded to the same scale. Bar, 2 cm.

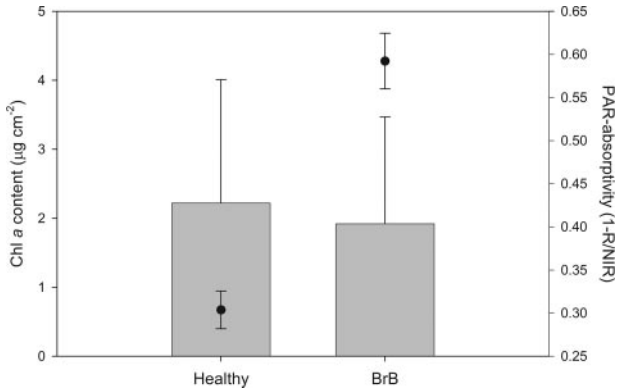


FIG. 3. Chlorophyll (Chl) *a* content (μg chlorophyll *a* cm$^2$ coral tissue surface area$^{-1}$) (gray bars) ($n = 3$) and PAR absorptivity (Abs = [1 − R/NIR]) (●) ($n = 4$) of healthy coral tissue and brown band tissue of *Acropora muricata*.

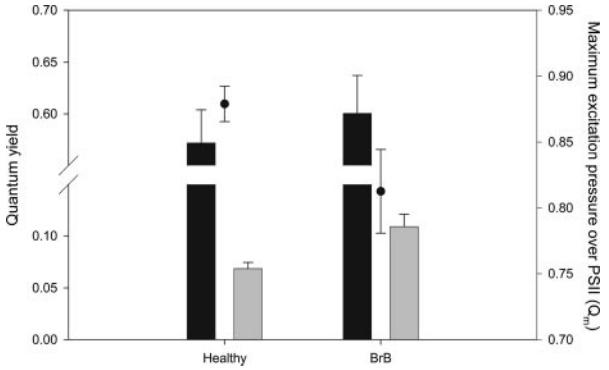


FIG. 4. Dark-acclimated maximum quantum yield ($F_v/F_m$) (black bars), high-light-acclimated effective quantum yield ($\Delta F/F_m'$) at 845 μmol photons $m^{-2}$ $s^{-1}$ (gray bars), and maximum excitation pressure over PSII ($Q_m$) at 845 μmol photons $m^{-2}$ $s^{-1}$ (●) ($n = 4$) of healthy coral tissue and brown band tissue (BrB) of *Acropora muricata*.

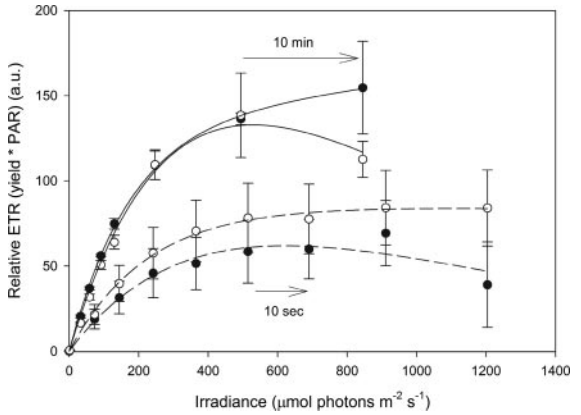


FIG. 5. rETR of dark-acclimated RLCs and SSLCs of healthy coral tissue (●) and brown band tissue (○) of *Acropora muricata*. Light-acclimated RLCs are not shown. Average values ($n = 4$) ± standard errors are given. The fitted rETR curves of RLCs and SSLCs are superimposed with a broken and a solid line, respectively. a.u., arbitrary units.

face area). This indicates that pigments were distributed differently between the healthy tissue and the brown band.

**Combined measures of variable chlorophyll *a* fluorescence and $O_2$ productivity.** Maximum quantum yield ($F_v/F_m$) and effective quantum yield ($\Delta F/F_m'$) as well as $Q_m$ of the fluorescence-derived dark-acclimated and light-acclimated RLCs are shown in Fig. 4. $F_v/F_m$ was unchanged ($P = 0.579$) between healthy (0.572 ± 0.032) and brown band (0.601 ± 0.037) tissue. $\Delta F/F_m'$ of healthy tissue (0.069 ± 0.006) was significantly lower ($P = 0.022$) than that of brown band tissue (0.109 ± 0.012). This relationship was reflected in subsequent calculations of the maximum excitation pressure over PSII ($Q_m$), which was higher (0.879 ± 0.013) in healthy tissue than in brown band tissue (0.813 ± 0.032), although the difference was not significant ($P = 0.102$) (Fig. 4).

The quantitative parameters of RLCs ($rETR_{max}$, α, and $E_k$) measured initially in the dark and again after increasing light exposure for 80 min were statistically compared to $rETR_{max}$, α, and $E_k$ calculated for fluorescence-derived SSLCs (Table 1). $rETR_{max}$ calculated for light- and dark-acclimated RLCs of healthy and brown band tissue showed similar values. However, the RLC performed on dark-acclimated brown band tissue also shared similar values with $rETR_{max}$ calculated for SSLCs of healthy tissue which were significantly different ($P = 0.003$). The $rETR_{max}$ calculated for SSLCs of brown band tissue was similar to values collected for all other groups of tissue and light curve types (Table 1). The slope of the rETR versus irradiance curves, α, showed similar values between healthy and brown band tissue within all three groups of light curves (Table 1). However, RLCs performed in the dark showed a significantly lower ($P = 0.011$) α than those calculated for SSLCs. α values calculated for RLCs performed in the light were similar to those for both dark-acclimated RLCs and SSLCs. There was no significant difference among groups of light curves and tissue types in minimum saturating irradiance, $E_k$ ($P = 0.571$) (Table 1; Fig. 5).

Healthy and brown band tissues exhibited widely different $O_2$ concentration levels over the entire irradiance range (Fig. 6). At the highest irradiance level (845 μmol photons $m^{-2}$ $s^{-1}$), the $O_2$ concentration of healthy tissue was 223 ± 4 μmol $liter^{-1}$ whereas the $O_2$ concentration of the brown band tissue was only 63 ± 22 μmol $liter^{-1}$. This amounts to ~30% of saturation $O_2$ concentration. In the dark, the $O_2$ concentration of the healthy tissue was 60 ± 28 μmol $liter^{-1}$ but virtually 0 (3 ± 3 μmol $liter^{-1}$) for brown band tissue due to high respiration activity coupled with $O_2$ transfer limitation imposed by the DBL (Fig. 6). The brown band tissue was almost completely hypoxic at irradiances below 60 μmol photons $m^{-2}$ $s^{-1}$ and never reached the compensation irradiance ($E_c$), i.e., the irradiance above which the tissue exhibits net oxygen production. The healthy tissue reached compensation irradiance at ~230 μmol photons $m^{-2}$ $s^{-1}$.

Microsensor measurements generally showed a thin DBL ranging from 100 to 200 μm and strong oxygen gradients across the DBL. Motility of the ciliates caused fluctuating oxygen signals, and this resulted in relative high variability in our flux

TABLE 1. Quantitative parameters derived from fitted rETRs of dark- and light-acclimated RLCs and SSLCs[a]

| Parameter | RLC (0) | | SSLC | | RLC (845) | | *P* |
|---|---|---|---|---|---|---|---|
| | Healthy | BrB | Healthy | BrB | Healthy | BrB | |
| $rETR_{max}$ | 83 ± 11$^{A}$ | 108 ± 4$^{A,B}$ | 172 ± 36$^{B}$ | 131 ± 15$^{A,B}$ | 71 ± 8$^{A}$ | 94 ± 22$^{A}$ | 0.003 |
| α | 0.39 ± 0.09$^{A}$ | 0.46 ± 0.05$^{A}$ | 0.69 ± 0.11$^{B}$ | 0.74 ± 0.06$^{B}$ | 0.49 ± 0.06$^{A,B}$ | 0.49 ± 0.05$^{A,B}$ | 0.011 |
| $E_k$ | 258 ± 79$^{A}$ | 243 ± 18$^{A}$ | 288 ± 85$^{A}$ | 179 ± 19$^{A}$ | 163 ± 45$^{A}$ | 196 ± 48$^{A}$ | NS |

[a] $rETR_{max}$ is in arbitrary units; α and $E_k$ are in μmol photons $m^{-2}$ $s^{-1}$. Numbers in parentheses after RLC are the irradiances applied (μmol photons $m^{-2}$ $s^{-1}$). Average values ($n = 4$) ± standard errors for healthy and BrB tissue are given. Values with different superscript capital letters were significantly different. NS, not significant.

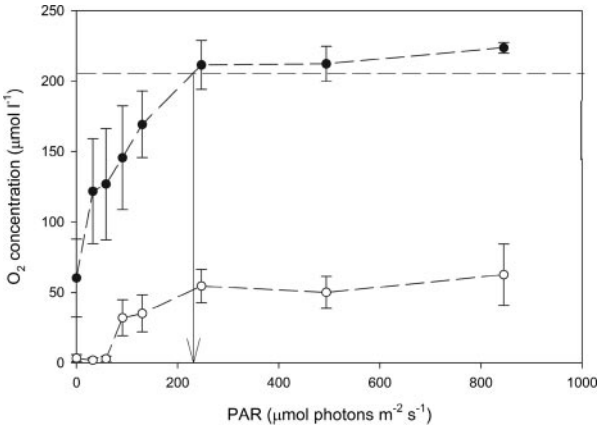


FIG. 6. Steady-state levels of $O_2$ concentration at the surface of healthy coral tissue (●) and brown band tissue (○) of *Acropora muricata* ($n = 4 \pm$ standard error) as a function of increasing irradiance (μmol photons $m^{-2}$ $s^{-1}$). The arrow indicate the compensation irradiance ($E_c$), above which the oxygen level at the tissue surface of healthy tissue exceeds the level of the overlying air-saturated seawater (204 μmol $liter^{-1}$).

calculations. Oxygen respiration rates in the dark were significantly different ($P = 0.011$) between healthy tissue ($0.22 \pm 0.04$ nmol $O_2$ $cm^{-2}$ $s^{-1}$) and brown band tissue ($0.48 \pm 0.05$ nmol $O_2$ $cm^{-2}$ $s^{-1}$) (Fig. 7). The compensation irradiance, $E_c$, i.e., the irradiance above which the tissue exhibits net oxygen production, was reached between 130 and 247 μmol photons $m^{-2}$ $s^{-1}$ in healthy tissue. However, maximum net production recorded beyond the compensation irradiance was low and highly variable ($0.15 \pm 0.09$ nmol $O_2$ $cm^{-2}$ $s^{-1}$). The brown band tissue exhibited net oxygen consumption at all irradiances, but consumption rates decreased with increasing irradiance, stabilizing around the $E_c$ determined for the healthy tissue (Fig. 7).

Although no net oxygen production was measured in the brown band tissue due to intense respiration, there was substantial gross photosynthesis (Fig. 8). There was no significant difference between quantitative parameters ($P_{g,max}$, α, and $E_k$)

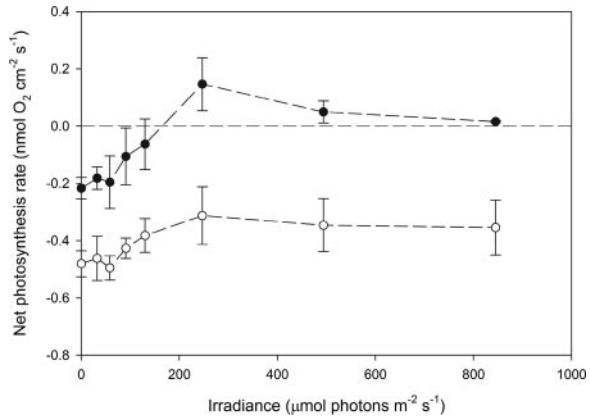


FIG. 7. Net photosynthesis rate (nmol $O_2$ $cm^{-2}$ $s^{-1}$) of healthy coral tissue (●) and brown band tissue (○) of *Acropora muricata* as a function of increasing irradiance (μmol photons $m^{-2}$ $s^{-1}$) of healthy and brown band tissue of *Acropora muricata* ($n = 3 \pm$ standard error).

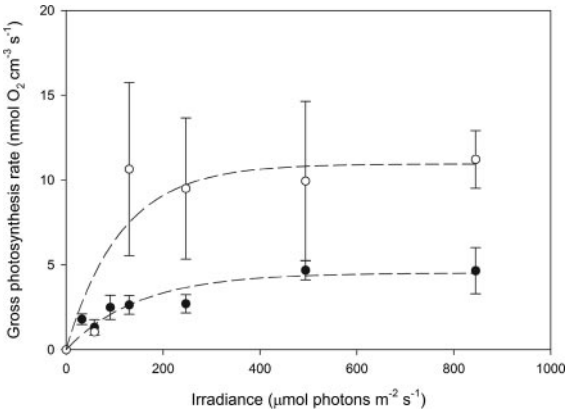


FIG. 8. Gross photosynthesis rate (nmol $cm^{-3}$ $s^{-1}$) of healthy coral tissue (●) and brown band tissue (○) of *Acropora muricata* as a function of increasing irradiance (μmol photons $m^{-2}$ $s^{-1}$) ($n = 3 \pm$ standard error). The fitted gross photosynthesis rate curve is superimposed with a broken line.

calculated from fitted gross photosynthesis rate and those calculated from irradiance curves (Table 2). Brown band tissue showed higher $P_{g,max}$ than healthy tissue (Fig. 8), although the difference was not significant ($P = 0.170$) (Table 2). There was no significant difference between healthy and brown band tissue in α ($P = 0.138$) or $E_k$ ($P = 0.517$) (Table 1).

## DISCUSSION

**Intact zooxanthellae in ciliates associated with BrB.** Reports concerning diseases of coral reef organisms have increased substantially over the last 2 decades (19, 28, 54). Coral diseases appearing with progressively greater frequency and wider distributions have been shown to alter total coral abundance and species diversity (20, 31, 44). A wide range of microorganisms including fungi, bacteria, cyanobacteria, and protozoans have been demonstrated to associate with both healthy and diseased corals (6, 15, 29, 30, 34, 41, 42, 43). BrB was recently described as a newly identified coral disease on the GBR. The distinctive macroscopic field symptom of BrB is the formation of a brown zone on the coral harboring high densities of motile yet unidentified protozoan ciliates (55). Although the prevalence of BrB on three reefs in the northern GBR was quite low, i.e., <1% of total number of coral colonies surveyed, corresponding to 12 to 24 cases per investigated reef (55), the high spreading rates and efficient transmission of BrB may cause significant damage to coral reef assemblages and can

TABLE 2. Quantitative parameters derived from fitted gross photosynthesis rate versus irradiance curves[a]

| Parameter | Healthy | BrB | *P* |
|---|---|---|---|
| $P_{g,max}$ | 5.37 ± 1.06 | 11.09 ± 3.11 | NS |
| α | 0.024 ± 0.007 | 0.065 ± 0.02 | NS |
| $E_k$ | 302 ± 120 | 204 ± 66 | NS |

[a] $P_{g,max}$ is given in nmol $O_2$ $cm^{-3}$ $s^{-1}$; α and $E_k$ are given in μmol photons $m^{-2}$ $s^{-1}$. Average values ($n = 3$) ± standard errors for healthy and brown band tissue (BrB) are given. NS, nonsignificant.

thus have large ecological impacts (B. Willis, personal communication).

Although other organisms such as bacteria and diatoms are also associated with the brown band zone of affected corals, the ciliates and ingested zooxanthellae account for the largest biomass. Light microscopy of the ciliates in the brown band tissue showed intact internal zooxanthellae with strong chlorophyll autofluorescence (Fig. 1B and C), lending support to the notion of photosynthetic competency of the zooxanthellae. The degeneration of symbiotic zooxanthellae in symbio is a routine process as cells divide and senesce (13, 14). Morphological changes associated with degeneration are characterized by vacuolization, disorganization of thylakoids, and enlargement of the accumulation body (5, 9, 13). Increased vacuolization in corals has previously been observed to result in loss of symbiont autofluorescence under green excitation light (13), but this was not observed in the grazed zooxanthellae investigated in this study. In addition, histological sections of ciliates also showed intact zooxanthellae within the cell cytostome (Fig. 1D) and without surrounding food vacuoles, which are otherwise indicative of the degradation of ingested food (18, 38). Our microscopic observations thus clearly showed that in BrB the ingested zooxanthellae are not degraded rapidly and remain intact within the ciliates.

**Photophysiology of ingested zooxanthellae.** Based on a novel methodological approach we showed that the zooxanthellae within the ciliates were photosynthetically competent. While microsensors for oxygen and variable chlorophyll *a* fluorescence have previously been employed separately to investigate the heterogeneity of zooxanthellar photosynthesis in hospite (25, 36), this study provides the first combined measurements of PSII quantum yields and derived rETRs together with measurements of steady-state $O_2$ concentration, rates of $O_2$ flux, and gross photosynthesis in diseased coral tissues. Our comparison between RLCs and SSLCs obtained from diseased corals is also novel. Our results show that SSLCs are different from RLCs, which delay only 10 to 20 s between each irradiance level. It is evident that if zooxanthellae are allowed to acclimatize for an extended period of time to each irradiance level, their photosynthetic performance yields higher rETR values. Thus, fluorescence-derived light curves obtained using PAM instruments are dependent on previous light exposure (see also reference 27).

**Pigmentation and optical properties.** Although the chlorophyll *a* content was similar across the disease lesion, the PAR absorptivity was significantly higher in the brown band zone (Fig. 2B and 3), suggesting that the light climate available to the zooxanthellae in this region was different from that of zooxanthellae associated with the healthy tissue. The higher absorptivity in the brown band indicates a more densely pigmented surface layer due to the high density of zooxanthella-containing ciliates in this zone. In healthy tissue, the pigments are distributed differently and primarily in the coral endoderm below the surface. The different tissue composition of the healthy and brown band zones invariably results in differing spectral properties and intensities of the light reaching the zooxanthellae in the two zones (10, 25). The paler tissue coloration in the healthy tissue (Fig. 1A) thus indicates a higher contribution of diffuse scattered light from the skeleton to the ambient light field of the zooxanthellae compared to the brown band tissue, and this will influence light-dependent measures of photosynthesis activity such as the effective quantum yield ($\Delta F/F_m'$) of PSII.

**Variable chlorophyll *a* fluorescence analysis.** There was no significant difference in $F_v/F_m$ between healthy and brown band tissue, indicating that PSII activity was not inhibited as a consequence of ingestion by ciliates (Fig. 2 and 4). Actually, the efficiency of light utilization, characterized by the effective PSII quantum yield, $\Delta F/F_m'$, apparently increased in zooxanthellae associating with ciliates.

Interestingly, the healthy tissue exhibited slightly lower rETR values throughout the irradiance range in dark-acclimated RLCs than did brown band tissue (Fig. 5), and this was mirrored in the gross photosynthesis irradiance curves (Fig. 8). Although the quantitative parameters of the RLCs are not significantly different (Tables 1 and 2), it is notable that the trend is reproduced across different techniques.

No photoinhibition, i.e., a decline in quantum yields or $O_2$ production measures at high irradiances, was observed except in the fluorescence-derived SSLC measures of healthy tissue (Fig. 5). The lack of significant differences in other fluorescence-derived light curves suggests that the photoinhibition observed is a reflection of a decrease in PAR absorptivity observed in healthy tissue that may cause higher scattering and light exposure (Fig. 3) (10).

**Oxygen dynamics.** The $O_2$ dynamics measured at the tissue surface showed a typical pattern of increasing $O_2$ levels, which saturated and approached a maximum value asymptotically with increasing irradiance for healthy tissue (Fig. 6). From such curves, the compensation irradiance, $E_c$, can be estimated as the irradiance at which there is no oxygen gradient across the DBL between the tissue surface and the surrounding water. At this irradiance there is no net exchange as oxygen consumption and production balance; above $E_c$ the system thus switches from being net heterotrophic to becoming autotrophic. In healthy tissue this occurred at a higher irradiance ($\sim$230 μmol photons $m^{-2}$ $s^{-1}$) than that previously reported for corals (25, 53), reflecting the fact that the corals were high light adapted (the *Acropora muricata* branches were from the reef flat) and thus exhibited a high respiration rate. In contrast, the brown band tissue demonstrated much lower $O_2$ concentration at the tissue surface, and oxygen levels at the highest irradiance reached only $\sim$25% of the $O_2$ concentration in the surrounding water due to high respiration of the ciliates and other constituents of the brown band tissue. In darkness and at the lowest irradiances, the brown band tissue was almost anoxic at the surface, indicating diffusion limitation of the oxygen supply across the DBL (Fig. 6). This limitation was clearly alleviated by the photosynthetic activity of the zooxanthellae at higher irradiance. Oxygen flux calculations for brown band tissue showed a net oxygen uptake, indicating that respiration was greater than gross photosynthesis at all experimental irradiances (Fig. 7).

Oxygen levels at the brown tissue surface were fluctuating due to the presence of highly motile and dense ciliate populations, and this caused high variability in our oxygen profiles. It is also possible that boundary layer compression due to the microsensor (see reference 16) affected our oxygen microprofiles and the derived oxygen fluxes. Finally, high densities of ciliates have previously been shown to affect the local transport

coefficient of oxygen (17), and if such enhancement was present in the brown band tissue it would affect our flux calculations. Advection induced by the ciliates could alleviate diffusion limitation significantly, as has been shown for large motile bacteria (12, 52). Enhancement of transport was shown to depend on both size and cell density of ciliates. For large filter-feeding ciliates such as *Euplotes* sp., it was shown that at cell densities above $10^3$ cm$^{-2}$ oxygen transport was significantly enhanced over the oxygen supply by diffusion alone (17). A zooxanthella-containing *Euplotes uncinatus* was recently described by Lobban et al. (30). A quantification of the ciliate density along with more detailed microsensor measurements and imaging of ciliate behavior would provide more insights into the mechanisms that affect oxygen fluxes in BrB, and our oxygen turnover rates reported here should thus be regarded as rough estimates. Nevertheless, the data clearly support our other data showing that zooxanthellae in the ciliates exhibit active photosynthesis.

**Photosynthesis in healthy versus brown band tissue.** The *A. muricata* branches sampled in this study were collected from a reef flat exposed to high irradiance, and as such the healthy tissue was visibly pale, indicative of a relatively low density of zooxanthellae in the coral tissue (Fig. 1A). The low net photosynthesis rates observed suggest that these high-light-exposed corals acquire necessary photosynthates from reduced zooxanthellar densities and thereby also reduce the risk of exposure to excess production of reactive oxygen species (32). In addition, the causative agent of BrB syndrome has not been determined, and it is unknown if the net photosynthesis production of healthy tissue preceding the brown band zone is compromised by a bacterial or viral pathogen. Pantos et al. (33) demonstrated that the bacterial community of the whole coral colony is affected even when just a small part of the colony shows signs of disease.

Results of gross photosynthesis measures (Fig. 8) confirm that the brown band tissue is indeed highly dynamic. The high variation observed in measurements, indicated by the large standard error, reflects the motility of the layer, which causes signal fluctuations even at steady state. The observed variation may also be due to variable health of the zooxanthellae, though this is unlikely since the PAM data do not support the assertion of compromised zooxanthellar health. Gross photosynthesis rates were higher, although not statistically significant, in the brown band tissue than in healthy tissue. Although the chlorophyll *a* contents of healthy tissue and brown band tissue were similar, the local density of zooxanthellae in the ciliates was enhanced, as seen in the higher absorptivity in the brown band tissue. Gross photosynthesis rate measurements with oxygen microsensors are influenced by the local density of active zooxanthellae around the tiny measuring tip, and this, along with a more efficient light capture, can explain the increased productivity in the brown band zone compared to healthy tissue. However, measurements of oxygen levels and fluxes showed that most of this productivity is channeled into respiration in the highly motile ciliate band.

**Ciliates with chloroplasts or photosymbionts.** Protozoa harboring photosymbionts are abundant in aquatic ecosystems (4, 11, 51) with mixotrophic (chloroplast-sequestering) oligotrich ciliates obtaining fixed carbon from photosynthesis as well as through ingestion of particulate matter (phagotrophy) (8). Species of oligotrichs in the genera *Tontonia*, *Laboea*, and *Strombidium* have been shown to enslave chloroplasts from ingested flagellates, and such kleptochloroplasts remain functional for periods ranging from hours to days fixing carbon that is metabolized by the ciliate (48, 49). However, kleptochloroplasts do not reproduce inside the ciliate and must therefore be constantly replaced through feeding. Such mixotrophic marine oligotrichs use photosynthesis primarily to cover respiratory demands and to increase their growth efficiency, but photosynthesis may also alleviate starvation when food is scarce (8, 50). To confirm such a survival strategy for brown band ciliates, life history studies of the ciliates are required.

Recently, the marine ciliates *Maristentor dinoferus* (Heterotrichea) and *Euplotes uncinatus* have been demonstrated to form associations with symbiotic zooxanthellae (29, 30). In the case of *Maristentor dinoferus*, approximately 50 to 800 dinoflagellates in the genus *Symbiodinium* clade C lineage have been observed within single ciliates (29). It is speculated that such ciliate-zooxanthella associations allow nutrients to pass from the ciliate to the dinoflagellate and photosynthates from dinoflagellate to the heterotrophic ciliate (30). Sommaruga et al. (47) detected UV-absorbing mycosporine-like amino acids in *Maristentor dinoferus* and proposed an additional mutualistic benefit of intracellular zooxanthellae, which in some cases are known to produce mycosporine-like amino acids (46). Whether similar UV protection occurs for ciliates in the brown band tissue requires a more detailed analysis of their pigmentation.

**Conclusion.** Our results show that zooxanthellae ingested by ciliates associated with BrB are photosynthetically competent and do not become compromised during the progression of the ciliate band. Ciliates feeding on coral tissue within the brown band tissue can thus gain additional energy from photosynthates and possibly alleviate oxygen limitation due to the photosynthesis of ingested zooxanthellae. Whether this association is a stable symbiosis or whether the zooxanthellae undergo a turnover and slow degradation in the ciliate, which requires constant uptake of new photosynthetically competent zooxanthellae, awaits further investigation.

## ACKNOWLEDGMENTS

We sincerely acknowledge David Abrego and A. Negri for laboratory assistance and Elizabeth Kulpa, Department of Primary Industries, Oonoomba Laboratories, Townsville, for performing histological preparation of samples. We thank G. Roff and B. Willis for valuable input and discussion during the preparation of the manuscript.

This work was performed in compliance with Australian laws and conducted under GBRMPA permit number G05/11866.1.

K. E. Ulstrup was supported by the Winifred Violet Scott Foundation. Additional support was from the Danish Natural Science Research Council.

This is contribution number 217 from the Institute of Water and Resource Management (IWERM).

## REFERENCES

1. **Antonius, A.** 1999. *Halofolliculina corallasia*, a new coral-killer ciliate on Indo-Pacific reefs. Coral Reefs **18:**300.
2. **Antonius, A., and D. Lipscomb.** 2001. First protozoan coral-killer identified in the Indo-Pacific. Atoll Res. Bull. **493:**1–21.
3. **Bancroft, J. D., and A. Stevens.** 1990. Theory and practice of histological techniques. Churchill Livingstone, Edinburgh, United Kingdom.
4. **Berk, S. G., L. H. Parkes, and R. S. Ting.** 1991. Photoadaptation alters the ingestion rate of *Paramecium bursaria*, a mixotrophic ciliate. Appl. Environ. Microbiol. **57:**2312–2316.

5. **Brown, B. E., M. D. A. Le Tissier, and J. C. Bythell.** 1995. Mechanisms of bleaching deduced from histological studies of reef corals sampled during a natural bleaching event. Mar. Biol. **122:**655–663.
6. **Cooney, R. P, O. Pantos, M. D. A. Le Tissier, M. R. Barer, A. G. O'Donnell, and J. C. Bythell.** 2002. Characterization of the bacterial consortium associated with black band disease in coral using molecular microbiological techniques. Environ. Microbiol. **4:**401–413.
7. **Cróquer, A., C. Bastidas, and D. Lipscomb.** 2006. Folliculinid ciliates: a new threat to Caribbean corals? Dis. Aquat. Org. **69:**75–78.
8. **Dolan, J. R., and M. T. Pérez.** 2000. Costs, benefits and characteristics of mixotrophy in marine oligotrichs. Freshw. Biol. **45:**227–238.
9. **Dunn, S. R., J. C. Bythell, M. D. A. Le Tissier, W. J. Burnett, and J. C. Thomason.** 2002. Programmed cell death and cell necrosis activity during hyperthermic stress-induced bleaching of the sea anemone *Aiptasia sp*. J. Exp. Mar. Biol. Ecol. **272:**29–53.
10. **Enriquez, S., E. R. Méndez, and R. Iglesias-Prieto.** 2005. Multiple scattering on coral skeletons enhances light absorption by symbiotic algae. Limnol. Oceanogr. **50:**1025–1032.
11. **Fenchel, T.** 1987. Ecology of protozoa. Science Tech Publishers, Madison, WI.
12. **Fenchel, T., and R. N. Glud.** 1998. Veil architecture in a sulphide-oxidizing bacterium enhances countercurrent flux. Nature **394:**367–369.
13. **Franklin, D. J., O. Hoegh-Gulberg, R. J. Jones, and J. A. Berges.** 2004. Cell death and degeneration in the symbiotic dinoflagellates of the coral *Stylophora pistillata* during bleaching. Mar. Ecol. Prog. Ser. **272:**117–130.
14. **Freudenthal, H. D.** 1962. *Symbiodinium* gen. nov. and *Symbiodinium microadriaticum* sp. nov., a zooxanthella: taxonomy, life cycle, and morphology. J. Protozool. **9:**45–52.
15. **Frias-Lopez, J., A. Zerkle, G. T. Bonheyo, and B. W. Fouke.** 2002. Partitioning of bacterial communities between seawater and healthy, black band diseased, and dead coral surfaces. Appl. Environ. Microbiol. **68:**2214–2228.
16. **Glud, R. N., J. K. Gundersen, N. P. Revsbech, and B. B. Jørgensen.** 1994. Effects on the benthic diffusive boundary layer imposed by microelectrodes. Limnol. Oceanogr. **39:**462–467.
17. **Glud, R. N., and T. Fenchel.** 1999. The importance of ciliates for interstitial solute transport in benthic communities. Mar. Ecol. Prog. Ser. **186:**87–93.
18. **Goff, L. J., and J. R. Stein.** 1981. Digestion in the peritrich ciliate *Ophrydium versatile*. Protoplasma **107:**235–254.
19. **Harvell, C. D., K. Kim, J. M. Burkholder, R. R. Colwell, P. R. Epstein, D. J. Grimes, E. E. Hofmann, E. K. Lipp, A. D. M. E. Osterhaus, R. M. Overstreet, J. W. Porter, G. W. Smith, and G. R. Vasta.** 1999. Emerging marine disease—climate links and anthropogenic factors. Science **285:**1505–1510.
20. **Harvell, C. D., C. E. Mitchell, J. R. Ward, S. Altizer, A. P. Dobson, R. S. Ostfeld, and M. D. Samuel.** 2002. Climate warming and disease risks for terrestrial and marine biota. Science **296:**2158–2162.
21. **Hasson, K. W., J. Hasson, H. Aubert, R. M. Redman, and D. V. Lightner.** 1997. A new RNA-friendly fixative for the preservation of penaeid shrimp samples for virological detection using cDNA genomic probes. J. Virol. Methods **66:**227–236.
22. **Hill, R., U. Schreiber, R. Gademann, A. W. D. Larkum, M. Kühl, and P. J. Ralph.** 2004. Spatial heterogeneity of photosynthesis and the effect of temperature-induced bleaching conditions in three species of coral. Mar. Biol. **144:**633–640.
23. **Hill, R., C. Frankart, and P. J. Ralph.** 2005. Impact of bleaching conditions on the components of non-photochemical quenching in the zooxanthellae of a coral. J. Exp. Mar. Biol. Ecol. **322:**83–92.
24. **Iglesias-Prieto, R., V. H. Beltran, T. C. LaJeunesse, H. Reyes-Bonilla, and P. E. Thome.** 2004. Different algal symbionts explain the vertical distribution of dominant reef corals in the eastern Pacific. Proc. R. Soc. Lond. B **271:** 1757–1763.
25. **Kühl, M., Y. Cohen, T. Dalsgaard, B. B. Jørgensen, and N. P. Revsbech.** 1995. Microenvironment and photosynthesis of zooxanthellae in scleractinian corals studies with microsensors for $O_2$, pH and light. Mar. Ecol. Prog. Ser. **117:**159–172.
26. **Kühl, M., R. N. Glud, H. Ploug, and N. B. Ramsing.** 1996. Microenvironmental control of photosynthesis and photosynthesis-coupled respiration in an epilithic cyanobacterial biofilm. J. Phycol. **32:**799–812.
27. **Kühl, M., R. N. Glud, J. Borum, R. Roberts, and R. Rysgaard.** 2001. Photosynthetic performance of surface associated algae below sea ice as measured with a pulse amplitude modulated (PAM) fluorometer and $O_2$ microsensors. Mar. Ecol. Prog. Ser. **223:**1–14.
28. **Lafferty, K. D., J. Porter, and S. E. Ford.** 2004. Are diseases increasing in the oceans? Annu. Rev. Ecol. Evol. Syst. **35:**31–54.
29. **Lobban, C. S., M. Schefter, A. G. B. Simpson, X. Pochon, J. Pawlowski, and W. Foissner.** 2002. *Maristentor dinoferus* n. gen., n. sp., a giant heterotrich ciliate (Spirotrichea: Heterotrichida) with zooxanthellae, from coral reefs on Guam, Mariana Islands. Mar. Biol. **141:**207–208.
30. **Lobban, C. S., L. Modeo, F. Verni, and G. Rosati.** 2005. *Euplotes uncinatus* (Ciliophora, Hypotrichia), a new species with zooxanthellae. Mar. Biol. **147:** 1055–1061.
31. **McClanahan, T. R., and N. A. Muthiga.** 1998. An ecological shift in a remote coral atoll of Belize over 25 years. Environ. Conserv. **25:**122–130.
32. **Nishiyama, Y., H. Yamamoto, S. I. Allakhverdiev, M. Inaba, A. Yokota, and N. Murata.** 2001. Oxidative stress inhibits the repair of photodamage to the photosynthetic machinery. EMBO J. **20:**5587–5594.
33. **Pantos, O., R. P. Cooney, M. D. A. Le Tissier, M. R. Barer, A. G. O'Donnell, and J. C. Bythell.** 2003. The bacterial ecology of a plague-like disease affecting the Caribbean coral *Montastrea annularis*. Environ. Microbiol. **5:** 370–382.
34. **Patterson, K. L., J. W. Porter, K. B. Ritchie, S. W. Polson, E. Mueller, E. C. Peters, D. L. Santavy, and G. W. Smith.** 2002. The etiology of white pox, a lethal disease of the Caribbean elkhorn coral, Acropora palmata. Proc. Natl. Acad. Sci. USA **99:**8725–8730.
35. **Platt, T., C. L. Gallegos, and W. G. Harrison.** 1980. Photoinhibition of photosynthesis in natural assemblages of marine phytoplankton. J. Mar. Res. **38:**687–701.
36. **Ralph, P. J., R. Gademann, A. W. D. Larkum, and M. Kühl.** 2002. Spatial heterogeneity in active chlorophyll fluorescence and PSII activity of coral tissues. Mar. Biol. **141:**639–646.
37. **Ralph, P. J., U. Schreiber, R. Gademann, M. Kühl, and A. W. D. Larkum.** 2005. Coral photobiology studied with a new imaging pulse amplitude modulated fluorometer. J. Phycol. **41:**335–342.
38. **Rasmussen, L.** 1974. Food vacuole membrane in nutrient uptake by Tetrahymena. Nature **250:**157–158.
39. **Revsbech, N. P.** 1989. An oxygen microelectrode with a guard cathode. Limnol. Oceanogr. **34:**474–478.
40. **Revsbech, N. P., and B. B. Jørgensen.** 1983. Photosynthesis of benthic microflora measured with high spatial resolution by the oxygen microprofile method: capabilities and limitations of the method. Limnol. Oceanogr. **28:** 749–756.
41. **Richardson, L. L.** 1997. Black band disease, p. 325–349. *In* E. Rosenberg and Y. Loya (ed.), Coral health and disease. Springer-Verlag, New York, NY.
42. **Rohwer, F., M. Breitbart, J. Jara, F. Azam, and N. Knowlton.** 2001. Diversity of bacteria associated with the Caribbean coral *Montastraea franski*. Coral Reefs **20:**85–91.
43. **Rohwer, F., V. Seguritan, F. Azam, and N. Knowlton.** 2002. Diversity and distribution of coral-associated bacteria. Mar. Ecol. Prog. Ser. **243:**1–10.
44. **Rosenberg, E., and Y. Ben-Haim.** 2002. Microbial diseases of corals and global warming. Environ. Microbiol. **4:**318–326.
45. **Schreiber, U.** 2004. Pulse-amplitude-modulation (PAM) fluorometry and saturation pulse method: an overview, p. 279–319. *In* G. C. Papageorgiou and Govindjee (ed.), Chlorophyll fluorescence: a signature of photosynthesis. Kluwer Academic Publishers, Dordrecht, The Netherlands.
46. **Shick, J. M., C. Ferrier-Pages, R. Grover, and D. Allemand.** 2005. Effects of starvation, ammonium concentration, and photosynthesis on the UV-dependent accumulation of mycosporine-like amino acids (MAAs) in the coral *Stylophora pistillata*. Mar. Ecol. Prog. Ser. **295:**135–156.
47. **Sommaruga, R., K. Whitehead, J. M. Shick, and C. S. Lobban.** 2006. Mycosporine-like amino acids in the zooxanthella-ciliate symbiosis *Maristentor dinoferus*. Protist **157:**185–191.
48. **Stoecker, D. K., M. W. Silver, A. E. Michaels, and L. H. Davis.** 1988. Obligate mixotrophy in *Laboea strobila*, a ciliate which retains chloroplasts. Mar. Biol. **99:**415–423.
49. **Stoecker, D. K., M. W. Silver, A. E. Michaels, and L. H. Davis.** 1989. Enslavement of algal chloroplasts by four *Strombidium* spp. Mar. Microb. Food Webs **3:**79–100.
50. **Stoecker, D. K., and M. W. Silver.** 1990. Replacement and aging of chloroplasts in *Strombidium capitatum* (Ciliophora: Oligotrichida). Mar. Biol. **107:** 491–502.
51. **Stoecker, D. K.** 1998. Conceptual models of mixotrophy in planktonic protists and some ecological and evolutionary implications. Eur. J. Protistol. **34:**281–290.
52. **Thar, R., and M. Kühl.** 2002. Conspicuous veils formed by vibrioid bacteria on sulfidic marine sediment. Appl. Environ. Microbiol. **68:**6310–6320.
53. **Ulstrup, K. E., P. J. Ralph, A. W. D. Larkum, and M. Kühl.** 2006. Intracolonial variability in light acclimation of zooxanthellae in coral tissues of *Pocillopora damicornis*. Mar. Biol. **149:**1325–1335.
54. **Williams, E. H., and L. Bunkley-Williams.** 1990. The world-wide coral reef bleaching cycle and related sources of coral mortality. Atoll Res. Bull. **335:** 1–71.
55. **Willis, B. L., C. A. Page, and E. A. Dinsdale.** 2004. Coral disease in the Great Barrier Reef, p. 69–104. *In* E. Rosenberg and Y. Loya (ed.), Coral health and disease. Springer-Verlag, New York, NY.
56. **Winkler, R., A. Antonius, and D. A. Renegar.** 2004. The skeleton eroding band disease on coral reefs of Aqaba, Red Sea. Mar. Ecol. **25:**129–144.